Mixture-Based Dielectric Permittivity Measurements Through Gallium-Excited Cavities

Anıl Karatay; Fatih Yaman

Published version information

Citation: A. Karatay and F. Yaman, "Mixture-Based Dielectric Permittivity Measurements Through Gallium-Excited Cavities," in *IEEE Transactions on Instrumentation and Measurement*, vol. 73, pp. 1-8, 2024, Art no. 6007808

DOI: https://doi.org/10.1109/TIM.2024.3428598

Mixture-based Dielectric Permittivity Measurements through Gallium-Excited Cavities

Anıl Karatay and Fatih Yaman *

Abstract

In dielectric measurements within resonant cavities, analytical perturbation methods encounter limitations, particularly with non-standard cavity shapes and lossy materials under test (MUTs) having high dielectric constant. In such cases, the demand for iterative techniques to improve accuracy and flexibility is evident, but the efficiency of existing iterative techniques, relying on numerical electromagnetic solvers, is often compromised, particularly in terms of time. Therefore, we introduce a novel methodology for measuring the permittivity of dielectric materials using liquid mixtures. This novel method employs a rapid iterative technique in which effective permittivity values are reconstructed at each iteration step based on the volume fraction of liquid mixtures, thus eliminating the dependence on time consuming 3D numerical solvers. Additionally, we aim to achieve dual-band measurements at 2.45 GHz and 5.8 GHz, enhancing precision by separating mode frequencies. Introducing a re-entrant cavity-like structure, we position the first mode at 2.45 GHz and the second at 5.8 GHz, effectively mitigating intermodal crosstalk and ensuring measurement accuracy. Also, for the first time in the literature, determining which mode will be excited in a cavity by the coupler probe made of gallium can be achieved through the displacement of the liquid metal which enables measurements to be taken exclusively at the desired frequency.

permittivity, cavity, liquid, perturbation, measurement

1 Introduction

The cavity perturbation technique is a widely employed approach for assessing the complex permittivity of materials in microwave frequencies [1]. It boasts numerous merits, including its simplicity, cost-effectiveness, non-destructive nature, speed, and versatility in measuring the permittivity of various materials, encompassing liquids, solids, and powders [2, 3]. Due to its notably high accuracy compared to other permittivity measurement methods and its capability

*The authors are with the Department of Electrical and Electronics Engineering, İzmir Institute of Technology, Urla, İzmir, 35430 Türkiye. F. Yaman is also with ASTeC, STFC Daresbury Laboratory, WA4 4AD Warrington, United Kingdom. e-mail: anilkaratay@iyte.edu.tr.

to effectively operate with small sample volumes [4], this method is frequently favored. Nonetheless, it may prove unsuitable for materials with high loss characteristics and the accuracy of this method can be influenced by factors like sample shape and size [5]. The arbitrariness of the sample or cavity shape necessitates the development of a new analytical model for each shape, which is often impractical for most structures [6, 7]. Furthermore, the cavity perturbation technique with analytical approach is usually limited to assessing complex permittivity at a single frequency.

Since the non-linear relationship between permittivity and resonant frequency can lead to inaccurate results when utilizing analytical methods alone, implementing iterative techniques is widely used to obtain accurate permittivity measurements. These methods can be applied to a diverse array of materials and are particularly useful for materials with complex dielectric properties. They involve solving systems that encompass both computed and measured frequency shifts, in conjunction with quality factor (Q) and power values. Newton–Raphson iterations in [8, 9] are enlisted to solve a system of equations, with Q, resonant frequencies or power, especially when the S-band cavity is loaded with samples. The approach proposed in [10], applicable to samples of arbitrary shapes, utilizes the Finite Element Method to numerically solve 3D non-homogeneous wave equations. Also examples exist in the literature where iterative methods are employed for in-situ measurements [11], but the measurements are time-consuming due to the numerical iteration process. The iteration process for permittivity measurement using microwave cavities requires specialized commercial software tools [8, 9, 11–13] or non-commercial numerical solvers [10]. To achieve accurate results via 3D numerical electromagnetic solvers, a full mesh simulation is required, and with each iteration step, these simulations need a high computational load for full mesh calculation. Beyond the challenges posed by inverse problems, frequency shifts and quality factor drops can occur during the measurement process, making it highly likely for modes to overlap in the frequency domain; thus, the mode frequencies must be sufficiently separated from each other to enable measurements across multiple frequency bands. Hence, innovative cavity designs are required because the desired level of separation cannot be achieved with conventional rectangular and cylindrical cavities. The adequate separation of mode frequencies in the frequency domain and having sufficient control over the excitation of modes prevent overlap in the relevant domain and significantly enhance measurement accuracy. Additionally, due to the lack of reconfigurable excitation capabilities for these modes in many coupler structures, unintended mode excitations can occur, significantly reducing measurement precision.

In this study, a novel mixture-based method for permittivity measurement with an iterative procedure is proposed, which overcomes the dependency on software tools. Instead of simulating the complex permittivity value at each step, it was adjusted by means of volume fraction through the ability to mix liquids. In the light of the complex dielectric information at various volume fractions for the reference liquids, it is feasible to determine the dielectric permittivity of an unknown material through the application of these referenced values. In this

manner, instead of conducting simulations which might take hours in modest systems at each step, the precise determination of the unknown MUT's complex dielectric permittivity can be achieved through a mixing process that will only take a few minutes. Specifically, well-documented ethanol-water mixture is used as a reference. By appropriately mixing these materials, when the frequency shift and Q reduction match those of the unknown material, the permittivity values of the respective material can be determined.

Another noteworthy innovation in this study is the implementation of the measurement process with a novel re-entrant cavity-like structure in a dual-band frequency range within the ISM bands, specifically at 2.45 and 5.8 GHz which are commonly utilized frequencies in WiFi, Wimax, WLAN and heating applications, with no other modes existing between the two frequencies placed as the first and second mode. This constraint, which cannot be resolved by conventional rectangular and cylindrical cavities [14], is circumvented by the novel cavity structure proposed in this study. The conventional cavities are structures where the maximum values for the first two mode ratios are 1.581 and 1.593, respectively. With the proposed structure, this ratio is extended to 2.37, aligning the first two modes at 2.45 GHz and 5.8 GHz. Importantly, this study achieves, for the first time in the literature, the production of such a cavity using a machining method, thus ensuring a more precise and accurate measurement. Furthermore, frequency switching and adjusting coupling factor are achieved through the manipulation of the shape and position of the probe, utilizing the liquid-metal displacement. To the best of our knowledge, this is also the first study to demonstrate that frequency switching and coupling factor adjustment in a microwave cavity can be accomplished through the liquid metal displacement. This paper introduces significant advancements in both measurement methodology and cavity design, coupled with an innovative excitation technique. It offers quite versatile, precise, rapid, and cost-effective approach for determining complex permittivity values.

2 Methods, Design and Fabrication

In this section, we provide a detailed account of the iterative process, the design and fabrication of the proposed cavity, and the excitation using liquid metal.

2.1 Iteration Procedure

The iterative procedure is built upon the task of determining the permittivity of an unknown material using known data. Essentially, two main options can be considered. The first involves the utilization of mixture models established in the literature to create a reference dataset, enabling the characterization of the unknown material's properties. The second option entails leveraging existing measurement results from the literature and undertaking a similar computational process. A plethora of models has been put forward in the academic sphere for determining the permittivity of liquid mixtures [15–19]. However,

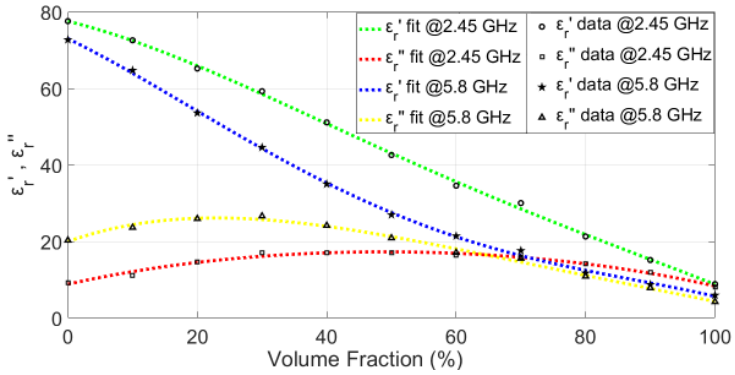

Figure 1: Room temperature dielectric properties of ethanol-water mixture at 2.45 GHz and 5.8 GHz

these models are highly idealistic and their applicability is rather limited for most mixtures. Due to the limited generalizability of mixture models to all mixtures, in this study, we opted for utilizing existing measurement data from the literature. As a proof of concept, the dielectric permittivities of an ethanol-water mixture at various volume fractions were employed as references at room temperature for frequencies of 2.45 GHz and 5.8 GHz. The ethanol-water mixture was selected for examination owing to its well-documented characteristics in the literature [20–23]; however, alternative liquid-liquid or liquid-powder mixtures with known dielectric properties can also be used.

Commencing with pure water and progressing in increments of 10% towards pure ethanol, the real and imaginary components of the dielectric permittivity are presented in Fig. 1. Here, the relative permittivity is denoted as $\varepsilon_r = \varepsilon_r^{'} - j\varepsilon_r^{''}$, where the real component can also be referred to as the dielectric constant. These data are fitted to fourth-order polynomials to approximate intermediate values. The measurement process unfolds as follows: Initially, the vector network analyzer is calibrated using the short, open, load, thru (SOLT) method, and the MUT is placed in a cavity with known resonance frequency and Q. The frequency shift and Q reduction caused by MUT are recorded for each mode. Subsequently, reference liquid mixtures, selected in this case as water and ethanol, undergo the same process, and the frequency shift and Q drop caused by water and ethanol in the respective modes are recorded. The subsequent goal is to align the frequency shift and Q drop for each mode with those induced by MUT. To achieve this, the reference liquids are mixed at varying ratios at each step, seeking a match with the values produced by MUT. The shift induced by MUT on the frequency and Q of the relevant mode in the cavity is measured in conjunction with a suitable holder; see Fig. 2. The measurements commence with two initial steps of the iteration process, starting with 100% ethanol and 0% ethanol (i.e., 100% water). The pure ethanol case and pure water case are considered as the initial guesses in Fig. 2. Subsequently, it continues with a 50%

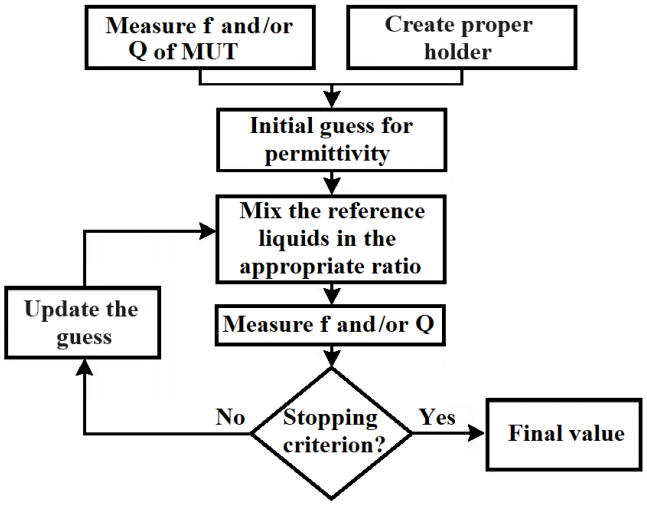

Figure 2: Flowchart of the proposed algorithm

ethanol volume fraction. Following this step, the iteration progresses with the bisection method toward 25% or 75%, depending on the frequency shift and Q drop induced by MUT. Throughout the article, each measurement step in this process is called iteration. The iteration is terminated if the difference between the frequency shift or Q drop value obtained during the measurements and that induced by the MUT is below the specified stopping criterion.

2.2 Cavity Design and Fabrication

The design process involved the insertion of two metallic cylinders into a cylindrical cavity with a diameter of 51.4 mm and a height of 26.5 mm from both the bottom and top surfaces. Assuming a cylinder diameter of 24 mm, various values of insertion length (L_{ins}) for the metallic cylinder were simulated. The study focused on examining the separation ratios of the first two modes and their corresponding frequencies under the assumption of a 24 mm cylinder diameter. It can be observed that the unperturbed cylindrical cavity exhibits its first mode at 4.46 GHz, while the second mode is at 6.6 GHz; see Fig. 3. The ratio of the resonance frequency of the second mode to that of the first mode is approximately 1.48. This ratio is below the analytically proven threshold of 1.593 in the literature, implying that surpassing this ratio is impossible as long as the cavity maintains its flawless cylindrical structure [14]. In the case where the metallic perturbation has dimensions of 10 mm, the first mode can be positioned at 2.45 GHz, and the second mode at 5.8 GHz. The crucial aspect here is the ability to achieve a frequency ratio of 2.37 between the first two modes. Once this ratio is achieved, accessing the relevant resonance frequency is again possible, thanks to the scalability of Maxwell's equations.

Since the measurement is desired to be conducted in the ISM bands as a

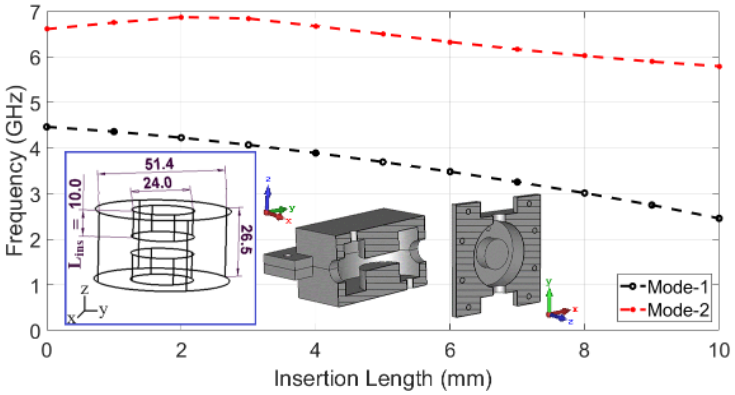

Figure 3: Effect of the insertion length on the design of the proposed cavity. The dimensions, yoz cross-section and xoy cross-section are provided in the bottom left, respectively.

dual-band configuration, the primary objective is to ensure that the modes are sufficiently separated in the frequency domain. The fundamental motivation behind the design of the structure is to place the first two modes at 2.45 GHz and 5.8 GHz, without leaving any other modes in between, in order to minimize the possibility of overlap of the modes on the frequency axis during permittivity measurement, due to different levels of frequency shifts and quality factor drops for each mode. The final form of the cavity was achieved using the Eigenmode solver in CST Microwave Studio. Although it may seem contradictory to the main motivation of the paper, only the initial design is presented here, allowing readers to perform dielectric constant measurements in the ISM band without the need for electromagnetic solver by using the proposed cavity directly. One seeking to employ this methodology for measurements may opt for another arbitrarily shaped cavity at a frequency of their preference. This flexibility arises from the method's inherent independence from the specific geometries of both the cavity and the sample.

In the measurement of dielectric permittivity, the locations of electric fields are of significant importance. The electric field vector arrows for the first two modes of the simulated cavity are displayed on two different cross-sections; see Fig. 4. The first mode, occurring at 2.45 GHz, is a TM_{010}-like mode associated with the cylindrical cavity, with the electric field peak situated at the center of the cavity. Meanwhile, the peak value of the electric field for the second mode is concentrated around the interior recess of the cavity. After the completion of the cavity design, manufacturing was carried out using two distinct conductive materials, namely steel and aluminum, through the machining process. In this production process, each cavity was constructed from two separate pieces and precisely aligned to be connected to each other with bolts as can be seen in Fig 5. Each piece features a total of eight bolt holes, which are correspondingly fastened to each other using bolts and nuts. The diameter of the bolt holes

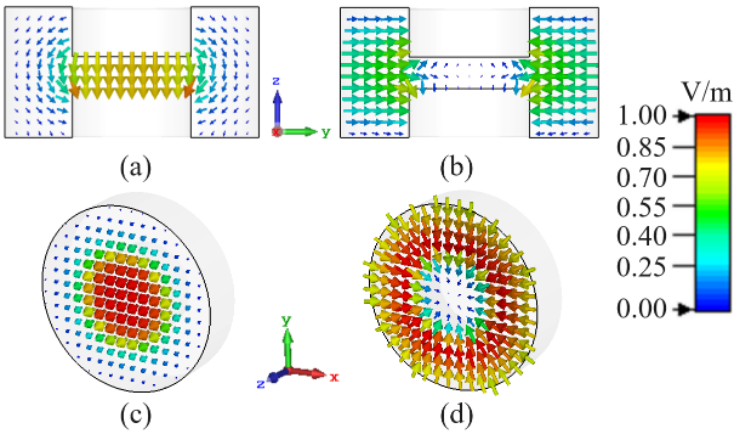

Figure 4: Normalized electric field vector arrows (a) Mode-1 yoz plane (b) Mode-2 yoz plane (c) Mode-1 xoy plane (d) Mode-2 xoy plane

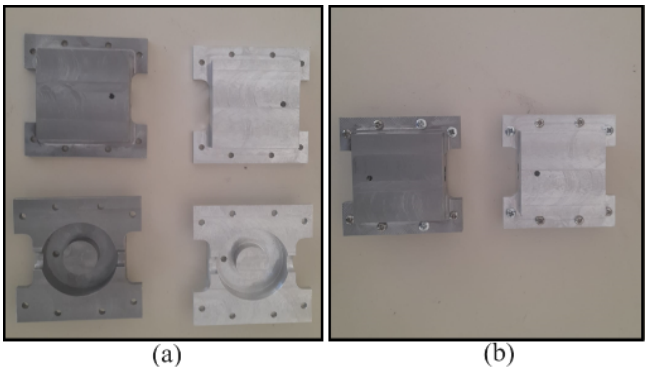

Figure 5: Fabricated cavities (The dark grey is steel and the light grey is aluminum) (a) unassembled pieces (b) assembled pieces

was chosen to be 4.2 mm, ensuring compatibility with M4-type bolts. At the intersections of the pieces, there are coupler holes with a combined diameter of 12 mm. The diameter of these coupler holes is designed to be suitable with N-type couplers, facilitating the dual-port excitation of the cavity. Each piece also features individual holes, each with a diameter of 4 mm, which can facilitate the insertion of frequency tuner during permittivity measurements if necessary.

2.3 Cavity Excitation

A resonant cavity can be modeled as a series RLC circuit connected to a transmission line with a characteristic impedance of Z_0. The unloaded quality factor (Q_0) and external quality factor (Q_{ext}) of the relevant mode of the cavity can

be expressed as follows.

$$Q_0 = \frac{\omega_0 R}{L},\ Q_{ext} = \frac{\omega_0 Z_0}{L} \tag{1}$$

where ω_0 denotes the angular resonant frequency of the relevant mode. R and L are the equivalent resistance and inductance, respectively.

When $Z_0 = R$, the equality of the unloaded quality factor and the external quality factor indicates critical coupling. The final form of the mathematical expression that relates these parameters is given by Equations 2, where the loaded quality factor, the measured quantity, is denoted as Q_L.

$$\frac{1}{Q_L} = \frac{1}{Q_0} + \frac{1}{Q_{ext}},\ \beta = \frac{Q_0}{Q_{ext}} \tag{2}$$

Given that the same coupler can generate different β values for different modes, MUTs or wall conductivities, it is necessary for the coupler to possess a reconfigurable property. For the first time, the technique of liquid metal displacement will be used to adjust the coupling coefficient of respective the modes of a cavity and to change the excited modes. Two different excitation states have been defined for the coupler, which, in turn, enable single-mode and dual-mode operation of the cavity. In addition, it is possible to adjust the coupling coefficient of the relevant mode by varying the amount of liquid metal. The parameter L_g shown in Fig. 6 represents the length of the liquid metal, and changes in this length affect both the coupling coefficients of the first and second modes. In simulations conducted with a 0.6 mm diameter metal, as the value of L_g increases, it is observed in Fig. 6 that the coupling of the first mode increases while that of the second mode decreases. In the experimental setup, achieving this condition is possible by filling the inside of a glass tube with liquid metal by using a syringe. If no liquid metal is added to the glass tube, the value of L_g will be zero, preventing the excitation of the first mode, thus achieving single-mode operation. In single-mode operation, a current is applied parallel to the electric field lines of the 5.8 GHz mode, while this current is orthogonal to the electric field vectors of the 2.45 GHz mode, thus not exciting the 2.45 GHz mode. Since the dielectric constant of the glass tube used is approximately 3.5, the tube's mere presence on its own will not have a significant impact on the excitation. On the other hand, in dual-mode operation, the interior of the glass tube attached to the coupler is filled, and a current parallel to the electric field vectors of the 2.45 GHz mode is also applied. This allows for the simultaneous excitation of both modes. As evident in Figure 7-(a), only the mode at 5.8 GHz is excited, while the mode at 2.45 GHz is suppressed. In the dual-mode operation measurement results shown in Figure 7-(b), both the modes at 2.45 GHz and 5.8 GHz are excited. The unloaded quality factor measured for the steel cavity at 2.45 GHz and 5.8 GHz was approximately 310 and 230, respectively, while in the aluminum cavity, it was measured at approximately 1800 and 1500 for the same frequencies.

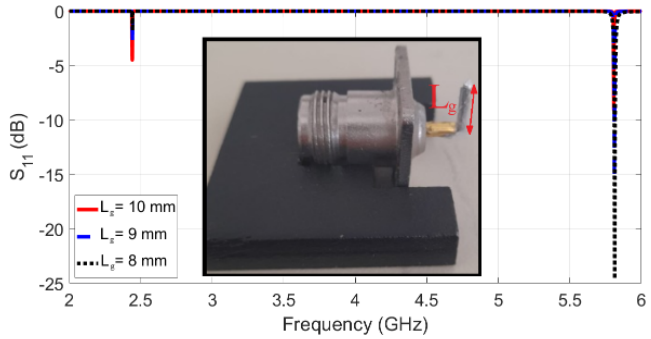

Figure 6: Liquid metal displacement-enabled coupler reconfiguration

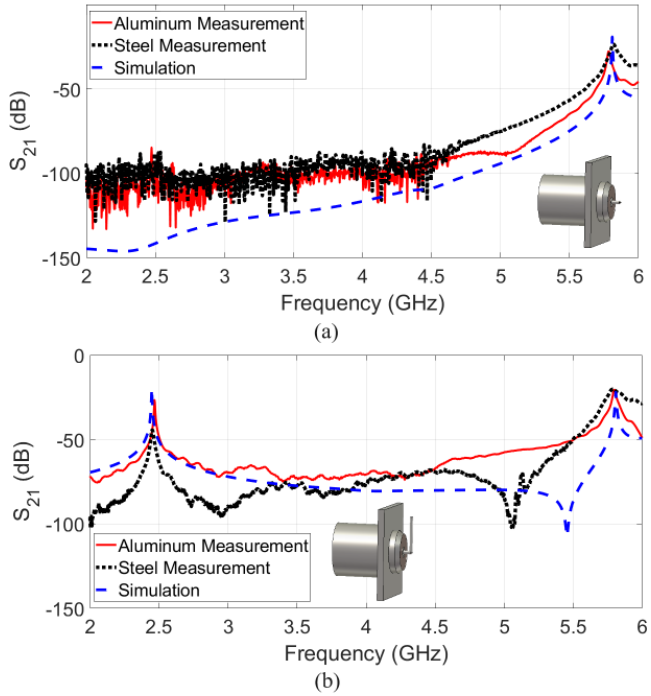

Figure 7: S_{21} results of the cavities (a) Single-mode operation (b) Dual-mode operation

3 Results and Discussions

In this section, dielectric characterization of two different materials, one liquid and one solid, was performed at 2.45 GHz and 5.8 GHz using the proposed method. Initially, two different holders, Sample 1 and Sample 2, were placed inside the cavity were positioned at the peak regions of the electric fields of the

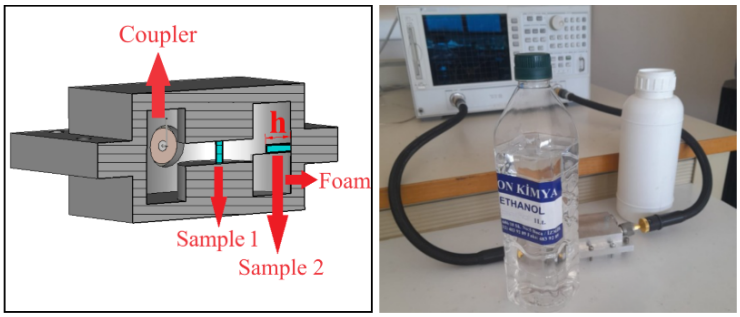

Figure 8: Experimental setup (a) model of the cavity and sample holders (b) liquids used in the iterative process

first and second modes; see Fig. 8. The change in resonant frequency of the relevant mode can be explained by perturbation theory given in Equation 3, which is dependent on the real component of permittivity. Hence, the uniqueness of the obtained dielectric constant from the measured frequency shift value is guaranteed. On the other hand, measuring the imaginary part is more complex because the quality factor is also a function of the frequency. Even if the imaginary components of the permittivities of two different materials are the same, when their real components differ, the resonance frequency of the cavity can vary significantly, resulting in different quality factor values. Therefore, the volumes and positions of the liquids placed inside the cavity are of great importance to ensure the uniqueness of the imaginary component.

$$\frac{f_s - f_{emp}}{f_{emp}} = \frac{-\int_{V_0}(\Delta\varepsilon'|\vec{E}|^2)dv}{\int_{V_0}(\varepsilon_0|\vec{E}|^2 + \mu_0|\vec{H}|^2)dv} \tag{3}$$

where f_s and f_{emp} denote the resonant frequency of the perturbed and unperturbed cavity, respectively. ε_0 and μ_0 are vacuum permittivity and permeability. $\Delta\varepsilon'$ indicates the change in the dielectric constant. Under the assumption that the sample placed in the cavity is nonmagnetic and of a small enough size not to alter the electric field pattern of the relevant mode, a relationship between the resonant frequency and the dielectric constant of the sample can be seen. Note that, the necessity of the iterative method becomes even more apparent with this equation because, when the cavity has an arbitrary shape, the electric field pattern and the corresponding volume integral cannot be precisely determined, and analytical calculations will result in errors. To confirm that a similar approach can be applied to the imaginary part, a series of simulations were conducted using the CST-MWS software with different permittivity values, and changes in the quality factor were examined. The real component of the sample's permittivity was incrementally raised from 5 to 65, and the quality factor change was tested with the imaginary permittivity values of 0.1, 0.2, 0.5, 1, and 10. In simulations, where the parameter "h" defined in Fig. 8-(a), was consid-

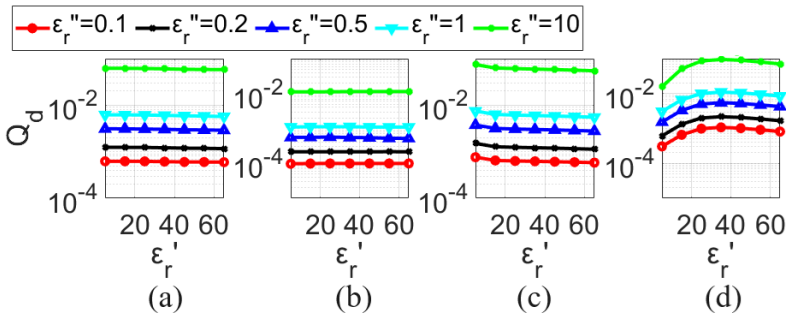

Figure 9: Applicability on imaginary permittivity reconstruction with varying holder lengths (h) (a) h = 8.7 mm at 2.45 GHz (b) h = 8.7 mm at 5.8 GHz (c) h = 22.6 mm at 2.45 GHz (d) h = 22.6 mm at 5.8 GHz

ered as 8.7 mm and 22.6 mm, the dependence of the change in quality factor due to imaginary permittivity on varying dielectric constant at both frequencies was examined; see Fig. 9. In the case of 8.7 mm, a linear response was observed at both frequencies, whereas when the holder length was increased to 22.6 mm, the same $\varepsilon_r^{''}$ value could lead to different changes in quality factor for different $\varepsilon_r^{'}$ values. Note that, $Q_d = (Q_{emp} - Q_s)/(Q_{emp}Q_s)$ where Q_{emp} and Q_s denote the unloaded quality factor of the empty cavity mode and that of the perturbed cavity, respectively. According to these results, if the sample volume is excessively large, two materials with different real parts of permittivity can create different Q_d values, even if they share the same imaginary part of permittivity. Therefore, adjusting the sample volume correctly emerges as a crucial factor. To verify this in the measurement setup, at 2.45 GHz, pure ethanol and pure water, despite differing dielectric constants, have equal imaginary components of permittivity. As a result, they should induce frequency shifts of different degrees, while the quality factor should shift by approximately the same. A similar process can be applied at 5.8 GHz, using pure water and a 50% ethanol-water mixture; check Fig. 1.

In the last step before the measurements, the applicability of the approach for both real and imaginary components was tested through full system simulations, and frequency domain analyses were conducted. The cavity structure was excited with a dual-port, and simulations were conducted using samples and holders with the dimensions provided above. The results are presented in Fig. 10. According to simulations for the compatible values of the ethanol-water mixture, if the real parts are the same and the imaginary parts are different, the same resonance frequency values with different Q values are obtained. Conversely, if the imaginary parts are the same and the real parts are different, different resonance frequencies with the same Q values are achieved.

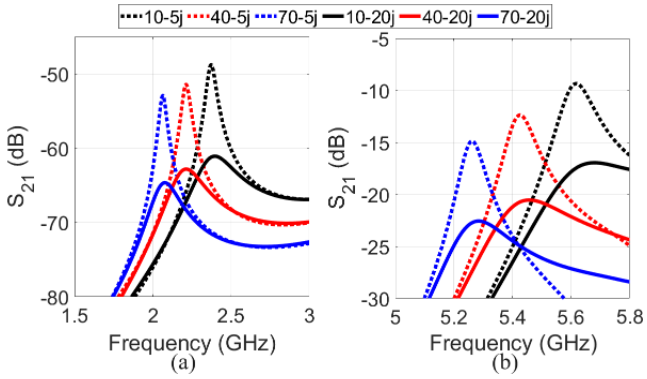

Figure 10: S_{21} simulations for the (a) first mode (b) second mode

3.1 Liquid Sample

Initially, the suitability of the holders' volumes and positions was checked with reference to ethanol-water mixtures, and experiments were commenced once it was confirmed that they were appropriate. Since the dielectric constant of the square prism holder with a inner edge length of 2 mm is approximately between 3-4 and it is made of a very thin material, it is not expected to significantly alter the measurement precision. After that, the MUT being a mixture consisting of 80% glycerin and 20% water was filled into the relevant holder and its frequency and quality factor variations in both modes were recorded. Subsequently, the MUT was completely removed, and an iterative matching process was attempted for frequency shifts and quality factor decreases at 2.45 GHz and 5.8 GHz using ethanol-water mixture with various volume fractions. The iterations, starting with pure water and pure ethanol, continued with a 50% volume fraction, and then, depending on the range of frequency shift and quality factor values of the MUT, were further pursued through the bisection method.

Due to the higher Q of the aluminum cavity, the S_{21} peaks or S_{11} dips are sharper compared to those in the steel cavity, making it possible to obtain the resonance frequency more accurately; see Fig. 11. On the other hand, measuring the Q is a more complex process than measuring the resonance frequency because it requires knowledge not only of the peak or dip points but also the half-power frequencies and coupling factors. This may not be distinguishable in the case of a low-Q. Therefore, while iterating the measurement of the imaginary part of permittivity in the steel cavity was not feasible, it was possible to measure and distinguish the quality factor in the aluminum cavity, despite the lossy sample. The actual result values in this figure were obtained from a dielectric characterization study of a glycerin-water mixture covering 2.45 GHz and 5.8 GHz frequencies available in the literature [24]. It is evident that the error rate, particularly in the real part of permittivity, is quite minimal. Larger discrepancies have surfaced in the imaginary part, attributable to factors such as the cavity's inadequate Q and variations in environmental conditions com-

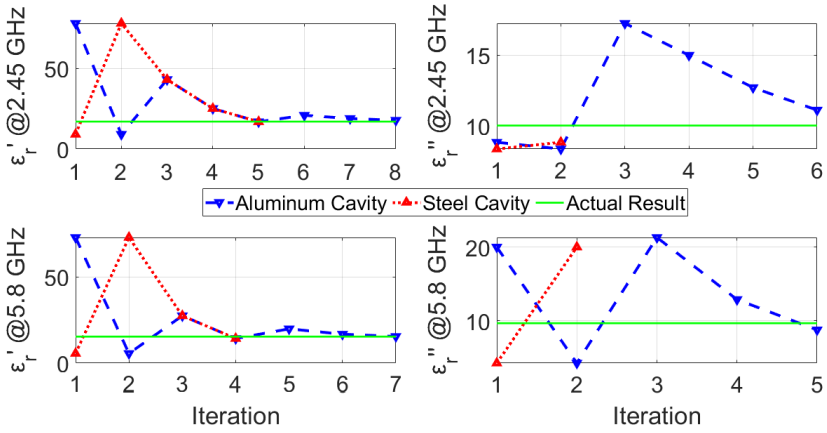

Figure 11: Iterative results of 80% glycerin by using ethanol-water mixture

pared to those in the literature. Nevertheless, the results are remarkably close to the actual values.

3.2 Solid Sample

To demonstrate the feasibility of measuring a solid sample using the similar approach, beef liver was taken as the MUT, and the same process was repeated. Beef liver used in the experiments was acquired from a food store in Türkiye. In this measurement, cylindrical holders with a 2 mm diameter and lengths as provided above were used instead of square prism holders, demonstrating that the measurement can be applied in different holder shapes. In the top right corner of Fig. 12-(a), there is a photograph depicting a liver placed inside the holder and without placement. The bottom side of the holder is sealed with silicone to prevent the sample and iteration liquids from overflowing outside the holder. The holder was first filled with beef liver, and then the iteration was conducted with ethanol-water mixture. Due to the inadequacy of the steel cavity's Q, the iteration for this material was exclusively performed with the aluminum cavity, as seen in Fig. 12, resulting in both real and imaginary components falling within the range of actual values at both frequencies. Permittivity values related to the liver can be found in various papers in the literature, but these values can vary depending on the water content inside the sample. Therefore, the Actual $\varepsilon_r^{'}$ and Actual $\varepsilon_r^{''}$ values were obtained within a range by referring to several sources [25–27].

3.3 Discussions

In the context of this work, the selected reference materials are water and ethanol, and our measurement range is constrained by the dielectric constants of these two materials. However, the literature contains numerous studies on

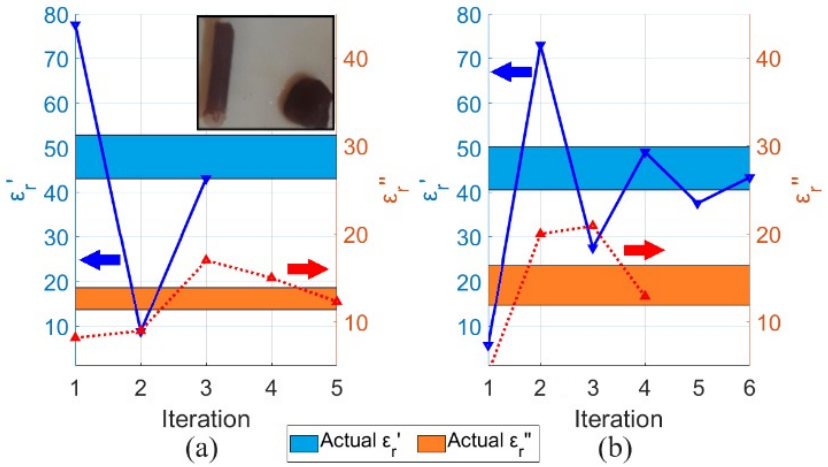

Figure 12: Iterative results of ex vivo beef liver in the aluminum cavity (a) 2.45 GHz (b) 5.8 GHz

mixture ratios of various materials (e.g. glycerin-water [24], methanol-water [28] etc.), and by selecting different mixtures, measurements can be conducted within varying dielectric permittivity ranges. While not obligatory for the base liquid to be water, it often emerges as a sound choice due to its relatively high dielectric constant, thereby expanding the measurement range.

As an alternative to this approach, one might explore concepts such as creating a look-up table that aligns frequency shift and dielectric constant. However, a fundamental challenge lies in the adaptability of such a table as the size and shape of the sample evolve, rendering it impractical. The proposed method has undergone testing with two distinct sample shapes, delivering successful outcomes for both solid and liquid samples. Notably, comparable results can be achieved even with a modest quantity of liquid sample occupying a fraction of the holder. Furthermore, in the case of the necessity to measure a solid sample that is incompatible with the holder's shape, the outer surface of the relevant solid sample can be modeled and produced using a 3D printer. The resulting 3D printed model can then be used as a holder, facilitating the iterative measurement process for the respective solid sample. Nevertheless, it should be noted that we do not have unlimited freedom in the dimensions of the sample and holder. A high imaginary permittivity of the sample broadens the S_{21} peak of the relevant mode and can complicate the determination of the resonance point. In the low-Q steel cavity, the premature termination of the iteration is attributed to the measurement of the real permittivity value. In the measurement of imaginary permittivity, ensuring that the frequency shift is sufficiently small and minimizing the dependence of the quality factor change on the real part of permittivity becomes crucial for accurate measurements. Additionally, the holder used may have a significantly larger dielectric con-

Table 1: Percentage error and Root Mean Square Error (RMSE) for the dielectric constant measurement of the glycerin-water mixture

Iteration	4	5	6	7	8
Mode-1 error (%)	43.4	-3.4	19.4	8.0	1.1
Mode-2 error (%)	-7.1	29.2	9.1	0.7	×
Mode-1 RMSE	0.3672				
Mode-2 RMSE	0.4571				

Table 2: Percentage error analysis for the dielectric constant of the beef liver

Iteration	3	4	5	6
Mode-1 error (lower actual) (%)	0.9	×	×	×
Mode-1 error (higher actual) (%)	-17.0	×	×	×
Mode-2 error (lower actual) (%)	-32.0	17.0	-7.4	6.9
Mode-2 error (higher actual) (%)	-45.2	-2.4	-25.2	-13.7

stant or imaginary permittivity compared to air, which can adversely affect measurement accuracy.

As we approach the final reconstructed value during the iteration process, the sampling rate of the VNA becomes a limiting factor, as minimal differences between frequency shifts caused by close permittivities become imperceptible. To achieve the result for 80% glycerin at 2.45 GHz and 5.8 GHz, six different measurements were taken at room temperature for each mode. For the 2.45 GHz measurements, four out of six was terminated at the 8th iteration step, while two measurement ended at the 5th step. Regarding the 5.8 GHz measurements, five out of six is terminated at the 7th iteration step, and one of them ended at the 4th iteration step. Measurements terminated at different iteration steps result in varying error rates, and these values are provided in Table 1. Since the measurement for the specific material is not terminated in the first three iterations, the error table started at the fourth iteration and calculated the RMSE values considering the error rates in all measurements taken. Additionally, temperature changes induced by environmental changes or electromagnetic sources have the potential to alter the dielectric constant of the sample, which can lead to early termination of the iteration. In this context, exciting the cavity with weak coupling instead of critical coupling increases the input power required for heating the sample inside and provides a more stable measurement environment. Moreover, minimal changes in the volume of the liquid filled in the holder and effects such as air bubbles can lead to premature termination of the iteration or directing it towards an erroneous point. However, experimental results have shown that such a situation does not lead to a high level of error. Similarly, when the percentage error analysis was conducted for the solid sample, the error rate was found relatively low; see Table 2. Since the actual value of the dielectric constant for liver is highly dependent on the moisture content, the provided value was not a single result but a range, and it was concluded that the beef

Table 3: Comparison of various cavity-based permittivity measurement systems (AP: Analytical Perturbation, IR: Iterative Resonant, INR: Iterative Non-resonant)

Ref.	[6]	[8]	[9]	[29]	[30]	Proposed
f_1 (GHz)	3.3	2.85	1.5	2.55	2.46	2.45
Size (λ^3)	0.088	0.609	0.210	0.064	0.198	0.027
Q	3800	NA	60	NA	233	1800
Type	AP	IR	INR	AP	AP	IR
3D Tool	No	Yes	Yes	No	No	No
ε'' Meas.	Yes	Yes	No	Yes	Yes	Yes
High ε'	No	Yes	Yes	No	No	Yes
Arb. Shape	No	Yes	Yes	No	No	Yes
Error in ε'	6.0%	10%	1.3%	5.2%	6.7%	1.1&0.9%

liver used in the study falls very close to the lower actual limit of the respective range by the obtained results.

Table 3 lists various cavity-based permittivity measurement methods, providing a comparison of their essential parameters. Since the lowest frequencies of the cavities in the table differ from each other, the sizes are given normalized to the longest operational wavelength and therefore their unit is λ^3. As mentioned above, the proposed method is an iterative approach, free from the limitations associated with high dielectric constants and the determination of the complex permittivity of arbitrarily shaped structures, which are fundamental challenges in analytical methods. Furthermore, transcending the inherent issue of time-consuming simulations in iterative approaches, it expedites the process by employing an experimental iteration method, thus significantly accelerating the procedure. The error rate of the proposed method, much lower than that of its analytical counterparts in the literature and comparable to iterative counterparts, opens the pathway for both accurate and expeditious measurements of complex permittivity.

4 Conclusion

In this paper, an iterative approach based on mixtures is proposed to address the limitations of the resonant cavity method with arbitrarily shaped cavities and samples, while preserving the high accuracy and capability to measure very small samples of the resonant cavity method. In contrast to other iterative techniques which employ 3D electromagnetic codes, the proposed approach eliminates the need for time-consuming simulations at each iteration step and removes dependence on commercial and non-commercial electromagnetic solvers. In order to achieve precise dual-band measurements in the ISM bands, a cavity with the first mode at 2.45 GHz and the second mode at 5.8 GHz has been proposed. This allows for mode separation in the frequency domain that can-

not be achieved with conventional cylindrical and rectangular cavities. These modes are flexibly excited through gallium, a liquid metal with a melting point of 29 °C, enabling versatile excitation and allowing for the adjustment of the desired coupling level based on the changing quality factor. This paper proposes significant innovations in both the measurement method and the cavity and excitation technique, providing a more flexible, low-error, rapid, and cost-effective means for the determination of complex permittivity compared to its cavity-based counterparts in the literature.

References

[1] C.-K. Kim, L. Minz, and S.-O. Park, "Improved measurement method of material properties using continuous cavity perturbation without relocation," *IEEE Trans. Instrum. Meas.*, vol. 69, no. 8, pp. 5702–5716, 2020.

[2] M. Barter, S. Partridge, D. R. Slocombe, and A. Porch, "Temperature correction using degenerate modes for cylindrical cavity perturbation measurements," *IEEE Trans. Microw. Theory Tech.*, vol. 67, no. 2, pp. 800–805, 2018.

[3] A. Verma and D. C. Dube, "Measurement of dielectric parameters of small samples at x-band frequencies by cavity perturbation technique," *IEEE Trans. Instrum. Meas.*, vol. 54, no. 5, pp. 2120–2123, 2005.

[4] A. La Gioia, E. Porter, I. Merunka, A. Shahzad, S. Salahuddin, M. Jones, and M. O'Halloran, "Open-ended coaxial probe technique for dielectric measurement of biological tissues: Challenges and common practices," *Diagnostics*, vol. 8, no. 2, p. 40, 2018.

[5] Z. Peng, J.-Y. Hwang, and M. Andriese, "Maximum sample volume for permittivity measurements by cavity perturbation technique," *IEEE Trans. Instrum. Meas.*, vol. 63, no. 2, pp. 450–455, 2013.

[6] A. Kik, "Complex permittivity measurement using a ridged waveguide cavity and the perturbation method," *IEEE Trans. Microw. Theory Tech.*, vol. 64, no. 11, pp. 3878–3886, 2016.

[7] J. Sheen and C.-M. Weng, "Modifications of the cavity perturbation technique for permittivity measurements of laminated samples," *IEEE Trans. Dielectr. Electr. Insul.*, vol. 23, no. 1, pp. 532–536, 2016.

[8] M. Santra and K. Limaye, "Estimation of complex permittivity of arbitrary shape and size dielectric samples using cavity measurement technique at microwave frequencies," *IEEE Trans. Microw. Theory Tech.*, vol. 53, no. 2, pp. 718–722, 2005.

[9] C. Özkal and F. Yaman, "A non-resonant approach for dielectric constant reconstructions via newton iterations," *AEU-Int. J. Electron. Commun.*, p. 154802, 2023.

[10] K. P. Thakur and W. S. Holmes, "An inverse technique to evaluate permittivity of material in a cavity," *IEEE Trans. Microw. Theory Tech.*, vol. 49, no. 6, pp. 1129–1132, 2001.

[11] R. Peter and G. Fischerauer, "In-situ measurement of permittivity distributions in reactors by cavity perturbation," *Meas. Sci. Technol.*, vol. 31, no. 9, p. 094019, 2020.

[12] C. Yu, Y. Tu, Y. Zhang, X. He, Y. Li, and E. Li, "An improved cavity-perturbation approach for simultaneously measuring the permittivity and permeability of magneto-dielectric materials in sub-6g," *IEEE Access*, vol. 9, pp. 14 807–14 815, 2021.

[13] A. K. Jha and M. J. Akhtar, "A generalized rectangular cavity approach for determination of complex permittivity of materials," *IEEE Trans. Instrum. Meas.*, vol. 63, no. 11, pp. 2632–2641, 2014.

[14] A. Karatay and F. Yaman, "Liquid Metal-Tunable Miniaturized Bimodal Cavity for Enhanced Measurement Accuracy in the ISM Bands," *IEEE Trans. Instrum. Meas.*, vol. 73, pp. 1–9, 2024.

[15] K. Thakur, K. Cresswell, M. Bogosanovich, and W. Holmes, "Modeling the permittivity of liquid mixtures," *J. Microw. Power Electromagn. Energy*, vol. 34, no. 3, pp. 161–169, 1999.

[16] E. Tuncer, Y. V. Serdyuk, and S. M. Gubanski, "Dielectric mixtures: electrical properties and modeling," *IEEE Trans. Dielectr. Electr. Insul.*, vol. 9, no. 5, pp. 809–828, 2002.

[17] K. K. Karkkainen, A. H. Sihvola, and K. I. Nikoskinen, "Effective permittivity of mixtures: numerical validation by the fdtd method," *IEEE Trans. Geosci. Remote Sens.*, vol. 38, no. 3, pp. 1303–1308, 2000.

[18] R. Clausius, *Die mechanische wärmetheorie*. Friedrich Vieweg und Sohn, 1879, vol. 2.

[19] M. A. Sarami, M. Moghadam, and A. G. Gilani, "Modified dielectric permittivity models for binary liquid mixture," *J. Mol. Liq.*, vol. 277, pp. 546–555, 2019.

[20] J.-Z. Bao, M. L. Swicord, and C. C. Davis, "Microwave dielectric characterization of binary mixtures of water, methanol, and ethanol," *J. Chem. Phys.*, vol. 104, no. 12, pp. 4441–4450, 1996.

[21] T. Sato and R. Buchner, "Dielectric relaxation processes in ethanol/water mixtures," *J. Phys. Chem. A*, vol. 108, no. 23, pp. 5007–5015, 2004.

[22] M. Palandoken, C. Gocen, T. Khan, Z. Zakaria, I. Elfergani, C. Zebiri, J. Rodriguez, and R. A. Abd-Alhameed, "Novel microwave fluid sensor for complex dielectric parameter measurement of ethanol–water solution," *IEEE Sens. J.*, vol. 23, no. 13, pp. 14 074–14 083, 2023.

[23] M. G. Mayani, F. J. Herraiz-Martínez, J. M. Domingo, R. Giannetti, and C. R.-M. García, "A novel dielectric resonator-based passive sensor for drop-volume binary mixtures classification," *IEEE Sens. J.*, vol. 21, no. 18, pp. 20 156–20 164, 2021.

[24] P. M. Meaney, C. J. Fox, S. D. Geimer, and K. D. Paulsen, "Electrical characterization of glycerin: Water mixtures: Implications for use as a coupling medium in microwave tomography," *IEEE Trans. Microw. Theory Tech.*, vol. 65, no. 5, pp. 1471–1478, 2017.

[25] H. Fallahi, J. Sebek, and P. Prakash, "Broadband dielectric properties of ex vivo bovine liver tissue characterized at ablative temperatures," *IEEE Trans. Biomed. Eng.*, vol. 68, no. 1, pp. 90–98, 2020.

[26] L. Abdilla, C. Sammut, and L. Z. Mangion, "Dielectric properties of muscle and liver from 500 mhz–40 ghz," *Electromagn. Biol. Med.*, vol. 32, no. 2, pp. 244–252, 2013.

[27] R. Balduino, B. McDermott, E. Porter, M. A. Elahi, A. Shahzad, M. O'Halloran, and M. Cavagnaro, "Feasibility of water content-based dielectric characterisation of biological tissues using mixture models," *IEEE Trans. Dielectr. Electr. Insul.*, vol. 26, no. 1, pp. 187–193, 2019.

[28] R. Smith Jr, S. Lee, H. Komori, and K. Arai, "Relative permittivity and dielectric relaxation in aqueous alcohol solutions," *Fluid Phase Equilib.*, vol. 144, no. 1-2, pp. 315–322, 1998.

[29] E. Kilic, U. Siart, O. Wiedenmann, U. Faz, R. Ramakrishnan, P. Saal, and T. F. Eibert, "Cavity resonator measurement of dielectric materials accounting for wall losses and a filling hole," *IEEE Trans. Instrum. Meas.*, vol. 62, no. 2, pp. 401–407, 2012.

[30] A. Karatay, H. Ö. Yılmaz, C. Özkal, and F. Yaman, "Cost-effective experiments with additively manufactured waveguide and cavities in the S-band," *Meas. Sci. Technol.*, vol. 34, no. 8, p. 085904, 2023.